International Journal of Pharmaceutics 434 (2012) 272–279

Contents lists available at SciVerse ScienceDirect

International Journal of Pharmaceutics

journal homepage: www.elsevier.com/locate/ijpharm

Exploring the effects of high shear blending on lactose and drug using fluidised bed elutriation

J.P. Willetts[a,*], P.T. Robbins[a], T.C. Roche[b], M. Bowley[c,d], R.H. Bridson[a]

[a] Centre for Formulation Engineering, School of Chemical Engineering, University of Birmingham, B15 2TT, UK
[b] GlaxoSmithKline, Research and Development, Inhaled Product and Device Technology Development, Park Road, Ware, Hertfordshire SG12 0DP, UK
[c] GlaxoSmithKline, Global Manufacturing and Supply, Priory Street, Ware, Hertfordshire SG12 0DJ, UK
[d] Ferring International Center S.A., Ch. de la Vergognausaz 50, 1162 Saint-Prex, Switzerland

ARTICLE INFO

Article history:
Received 23 January 2012
Received in revised form 4 May 2012
Accepted 15 May 2012
Available online 6 June 2012

Keywords:
Dry powder inhaler
High shear blending
Lactose
Fluidisation
Elutriation

ABSTRACT

Powder formulations comprising inhalation grade lactose and a mimic drug (cholesterol) were prepared using a high shear blending process for which the total energy input could be quantified. The formulations were fluidised in a classic fluidised bed system, to determine whether blending-induced changes could be determined through either bulk fluidisation behaviour or the characteristics of elutriated fractions from the powder beds. The evolution of the fluidisation regime within the powder beds (Δ pressure vs. superficial gas velocity) and total mass of elutriated material were not sensitive measures to differentiate between blended and unblended samples. However, blended and unblended material could be distinguished by the size distributions of the elutriated fractions. The study also showed that there were no further changes in the size distribution of the elutriated fractions once a chemically homogenous mixture of lactose and drug had been produced. However, further blending beyond this 'point of homogeneity' continued to change the lactose particle size distribution of the bulk powder; this may have implications for blend end point determination for these types of formulation.

1. Introduction

Over recent years, the pharmaceutical industry has placed increasing importance on understanding the relationship between pharmaceutical manufacturing processes and the quality and functionality of the products that they produce. In the spirit of this principle, previous work has investigated how a high shear blending process, representative of a secondary manufacturing operation used to make dry powder inhaler (DPI) formulations, affected the properties of the widely used inhalation excipient, α-lactose monohydrate (Bridson et al., 2007). Key findings included the relationship between cumulative energy input and particle size distribution and a change in surface material characteristics at high-energy input. Continuing from this work, the aims of this study were to:

(i) further explore the impact of high shear blending on lactose and lactose/drug mimic systems and the effect this may have on DPI performance and

(ii) explore the use of a fluidised bed as a potential tool for blend characterisation.

The main hypothesis is that processing the blended powder in a fluidised bed and analysis of the resulting fluidisation and elutriation behaviour can be used to distinguish between blended and unblended material and thus act as a post-blending test.

Fluidised beds are widely used throughout the process industries for operations such as mixing, drying, reaction and granulation (Davidson et al., 1985; Kunii and Levenspiel, 1991). The term "fluidised" refers to the fact that a bed of solid particles within the system can be seen to move in a fluid-like fashion as an upwards stream of gas is passed through it at sufficient velocity for the frictional losses (measured as a pressure drop) to overcome the weight of the bed. In conjunction with the operating parameters and equipment design, the properties and characteristics of the particles in the fluidised bed system are well known to influence the type of fluidisation behaviour and related aspects such as entrainment (flux of solids away from the bed, carried in the airstream) and elutriation (the subsequent classification and removal of entrained particles from the system). While elutriation of particles from a fluidised bed is often an undesirable phenomenon leading to material depletion and dust, its classification effect can be exploited. For example, Santana et al. (1999) and Mahmoud

* Corresponding author.
E-mail address: johnwillettsresearch@gmail.com (J.P. Willetts).

0378-5173/$ – see front matter © 2012 Elsevier B.V. All rights reserved.
http://dx.doi.org/10.1016/j.ijpharm.2012.05.032

et al. (2004) investigated separation of fine inorganic particles (typically ~0.5–5 μm) from larger coarse particles (~50–400 μm) by fluidised bed elutriation. Santana et al. showed that fines in such systems exist as either free particles, small agglomerates with each other, or agglomerates with larger particles. Mahmoud et al., also showed that fines exist as different entities and stated that elutriation from the fluidised bed is affected by interparticle adhesion forces. In a recent pharmaceutical example, the principles of fluidised bed elutriation have been used to mimic the air-induced segregation effects observed in a tablet press during direct compression through a vertical chute (Deng et al., 2010).

In the dry powder inhaler literature, the use of the terms *fluidisation* and *entrainment* are often used when describing the events occurring during the inhalation process i.e. the aerodynamics of transferring powder from device to airways over the course of milliseconds. For example, in their extensive evaluation of characterisation techniques for DPI formulations, Hickey et al. (2007) state how fluidisation of powder is a necessary step during inhalation and that this state can be achieved once momentum overcomes interparticulate forces. Tuley et al. (2008) passed high velocity airstreams through powders residing in reservoirs of different geometries, reporting their behaviour in terms of fluidisation and entrainment. Shur et al. (2008) reported the effects of different powder treatments using fluidisation as a potential analogy to explain observed effects. Here, we investigate whether the behaviour of powders subject to an industrially relevant blending process can be explored using a classic fluidised bed system, with particular emphasis on elutriation.

2. Materials and methods

2.1. Materials

Inhalation grade lactose (d_{50} ~70 μm) was obtained from Friesland Foods Domo, Netherlands. Samples of this material used throughout the study were taken from batches stored at 20 °C and 40% RH in a humidity-controlled cabinet (Binder, Germany) unless stated otherwise.

All solvents (propan-2-ol for particle size measurements and octane for surface area studies) used in material analysis were of analytical grade, purchased from Fisher Scientific (Loughborough, UK) and used as received.

Cholesterol was used as a mimic drug and was purchased from Sigma–Aldrich (Dorset, UK). Micronisation of the original material was performed in a planetary ball mill with a 45 ml grinding bowl (Pulverisette 6, Fritsch, Germany). Briefly, micronisation conditions were as follows: solid:liquid ratio 1:3, grinding media 1 mm zirconium oxide beads, 2 h run time at 400 rpm, bowl filled to top to prevent "foaming" of material (Czekai and Seaman, 1999). Following micronisation, light microscopy showed the particles to have a narrow size distribution and average diameter of approximately 3 μm. Wet laser diffraction analysis (Mastersizer 2000, Malvern Instruments, UK) gave a d_{50} of approximately 4 μm when a few drops of surfactant (1%, v/v polysorbate 20) were added to enhance the dispersion of particles.

2.2. High shear blending

High shear blending equipment as previously described in Bridson et al. (2007) was used. Key features included a cylindrical, stainless steel bowl (with lid), with a flat base, vertical side walls and internal diameter of 0.13 m. The bowl was mounted on bearings so that it would have been free to spin if it had not been prevented from doing so by a force transducer that provided a measurement of the instantaneous torque on the bowl (Knight et al., 2001). The power input, P(W) into the powder during blending could be related to this force via Eq. (1):

$$P = \frac{2\pi RFN}{60} \quad (1)$$

where R (m) is the distance from the central axis of rotation to the force transducer, F (N) is the force measured by the transducer and N (rpm) is the rotational speed of the blade. The force measured was dependent upon the blade speed (N) and mass of powder in the bowl, with normally an increase in speed or mass leading to a higher force. The energy input E (J) between times t_1 and t_2 could then be found from:

$$E = \int_{t_1}^{t_2} Pdt \quad (2)$$

A constant blade speed of 500 rpm and bowl fill of 500 g were employed for all experiments; therefore the total energy input to the powder during blending was dependent on the blend time i.e. the longer the blend, the higher the energy input.

For blending experiments in which cholesterol was used, batches were prepared by filling the bowl in a stratified manner, with three equal layers of drug sandwiched between four equal layers of lactose. As each successive level was added, the powder was levelled by gently shaking the bowl. The total amount of drug added to 500 g of lactose was 7.3 g (1.46%, w/w). Sampling to determine drug content of blends and to provide material for particle size analysis was performed at 20 vertically and radially different locations throughout the bowl. From each sample, 34.25 mg was taken for drug content analysis, corresponding to dosage of ~500 μg. Drug content was quantified using UV spectrophotometry (V-530 UV/Vis Spectrophotometer, Jasco, UK) at λ_{max} = 205 nm against a standard curve ($R^2 > 0.99$). Cholesterol content homogeneity was defined when the coefficient of variation across the 20 samples was found to have reduced to 5–6%, in line with other studies in the field (Flament et al., 2004; Saint-Lorant et al., 2006; Thi et al., 2008).

2.3. Fluidised bed design

2.3.1. Dimensions

Fig. 1(a) shows a schematic illustration of the fluidised bed system (FBS) used in this study. Initial scoping studies found that around 20 g of material in the fluidised bed gave sufficient elutriated material to test. As a suitable bed height, H, to diameter ratio, D, is 2 (H/D ~2) and lactose powder has a bulk density of ~ 700 kg m^{-3} this led to a circular internal diameter of 25 mm for the FBS column. The column height was 450 mm, chosen by considering the transport disengagement height (TDH) and how this relates to particle elutriation (Section 2.3.3).

2.3.2. Operating flow rate

Particles can only be elutriated when the superficial gas velocity through the bed exceeds their terminal velocity. Therefore, the flow rate used during an experiment will affect the particle size fraction elutriated. The bed had a fairly broad particle size distribution; in the initial scoping studies it was found that a cut size of around 25 μm (i.e. elutriation of particles below this size) was suitable as this provided sufficient material for analysis.

Application of Stokes' law (Eq. (3)), allows the terminal velocity of particles to be approximated for systems with low Reynolds number (Re < 1). This was considered a sufficiently good starting point for the necessary calculations, despite its limitations (e.g.

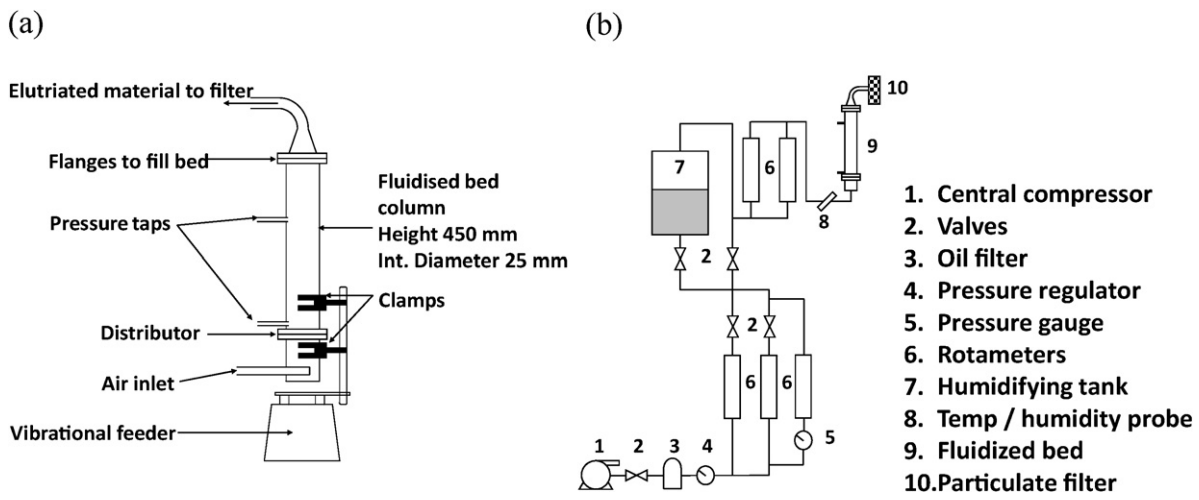

Fig. 1. Schematic illustration of (a) the vibrating fluidised bed and (b) the air humidification rig.

assumptions relating to particle shape are not met by the powders used in this study):

$$U_t = \frac{d_p^2(\rho_p - \rho_g)g}{18\mu} \quad (3)$$

where U_t is the terminal velocity ($m\,s^{-1}$), g is the acceleration due to gravity ($m\,s^{-2}$) d_p is the particle diameter (m), ρ_p and ρ_g are the densities of the particle and gas respectively ($kg\,m^{-3}$), and μ is the gas viscosity ($kg\,m^{-1}\,s^{-1}$ Pa s).

For a cut size of 25 μm, the minimum required gas velocity was found to be ≈3 cm s^{-1} (based on $\rho_p \sim 1500\,kg\,m^{-3}$, $\rho_g \sim 1.2\,kg\,m^{-3}$, $\mu \sim 1.7 \times 10^{-5}$ Pa s). Based on the recommendation that during air classification by fluidised bed elutriation, the fluidising velocity should be at least twice the terminal velocity of the fines cut size (Heath and Aconsky, 1963), a gas velocity corresponding to a volumetric flow rate of 2 l min^{-1} was chosen (6.8 cm s^{-1}). This volumetric flow rate was convenient to measure on the rotameters.

2.3.3. Transport disengagement height

The available transport disengagement height (TDH) should be such that coarse particles initially entrained in the air stream have the opportunity to return to the bed rather than being elutriated. Above the TDH, only the desired fraction remains entrained and so is elutriated from the bed. Equations for estimating the TDH are available in the literature for different particle systems e.g. Zenz and Weil (1958), Smolders and Baeyens (1997) and Kunii and Levenspiel (1991). The experimentally derived relationship of Fournol et al. (1973) (Eq. (4)) was used for this work as their catalytic particle system had a similar average particle size and, like the lactose used in this study, was difficult to fluidise.

$$\frac{U_{sgv}^2}{\mathrm{TDH}g} = 0.001 \quad (4)$$

Where U_{sgv} is the superficial gas velocity, TDH is the transport disengagement height and g is acceleration due to gravity. Based on the chosen superficial gas velocity of 6.8 cm s^{-1}, the TDH necessary from Eq. (4) is approximately 450 mm.

2.3.4. Other key features and equipment

The distributor was made from filter paper (Grade 1 Qualitative Cellulose Filter Paper (Whatman, UK). A stainless steel filter unit containing a sintered thimble (Swagelok, part number: SS-12TF-MM-05, 0.5 μm pore size) downstream of the bed exit allowed collection of elutriated particles. After each experiment the thimble could be removed to allow sample weighing and other analyses. Due to the cohesive nature of the lactose (this grade of inhalation lactose is a mixture of Geldart group A and C powders (Geldart, 1973)), the bed was gently vibrated to reduce channelling and plug formation (Jaraiz et al., 1992; Mawatari et al., 2003; Levy and Celeste, 2006) using a small vibrational feeder (Retsch Vibratory Feeder DR 100) with oscillations of 40 Hz, and amplitude 1 mm.

The fluidising gas was air supplied by a compressor. This was filtered and humidified before entering the column (Fig. 1 (b)). The air humidity was controlled by a valve situated on a bypass line across a humidifying tank of water. The temperature and humidity of the fluidising air were manually maintained at 40 ± 5% RH and 20 ± 2 °C, respectively, recorded with a temperature and humidity sensor (HumidiProbe) and data logging software (both from PicoLog, Pico Technology Ltd., UK). This humidity was maintained as a compromise to both minimise the agglomeration that could be caused by high humidities (Bridson et al., 2007), and reduce the electrostatic forces associated with low humidities that could affect fluidisation and elutriation (Park et al., 2002). Volumetric flow rates were measured and controlled by rotameters, and pressure drop measurements were recorded using a digital manometer (FC0510 Micromanometer, Furness Controls Limited, UK).

2.4. Material characterisation

2.4.1. Particle size distribution

To determine particle size distributions, laser diffraction particle sizing techniques were used; 'dry' for exploring agglomeration behaviour and 'wet' where primary particles were of interest. For dry analysis, A HELOS/BF detector was used in conjunction with a RODOS/L dispersion unit (Sympatec, Germany). Measurements were performed at a dispersion pressure of 2 bar using a R3 lens with focal length 100 mm and 0.5–175 μm detection range. Wet dispersion analysis was performed with a Malvern Mastersizer 2000 (Malvern Instruments Ltd., UK) using the 300 RF lens and the small volume sample dispersion unit (capacity 150 ml) operating at 1200 rpm. Lactose samples were suspended in propan-2-ol (Adi et al., 2007), and added drop-wise to the dispersion unit containing 150 ml propan-2-ol until an obscuration of between 15 and 18% was achieved. Refractive indices of 1.533 and 1.378 were used for lactose and propan-2-ol respectively, with an estimated imaginary refractive index for lactose of 0.1.

2.4.2. Specific surface area

Specific surface area measurements were performed using a DVS Advantage II (Surface Measurement Systems, UK) through

application of the Brunauer Emmet Teller (BET) equation to adsorption data obtained using octane as a probe molecule. This is an alternative to a nitrogen gas adsorption method. Dry oxygen-free nitrogen was purged over the 120 ± 5 mg sample for 4 h. The partial pressure was then sequentially increased from 0 to 96% in 3% increments, with the sample being allowed to reach a near-equilibrium (% dm/dt = 0.0002% min^{-1}) at each partial pressure stage before progressing to the next. All stages of the experiment were performed at 25 ± 0.1 °C.

2.4.3. Cohesivity

Cohesivity of materials was determined using a Ring Shear Tester, (RST-XS, Dr. Dietmar Schulze, Wolfenbüttel, Germany). A small volume of material (~30 cm^3) was loaded into a shear cell with the excess powder scraped off by a spatula, ensuring that negligible force was applied to the powder surface. The powder was then weighed before a lid was placed on top of the bed and a loading rod inserted to apply the normal stress to the bed. Two tie rods were then used to apply a shear stress, attached to two load cells. To test the cohesivity of materials used in this study, a preshear stress of 20 kPa was applied before consolidation stresses of 2, 3, 5, 10, 15 kPa to determine at which points the bed failed. These values were chosen to correspond to consolidation stresses experienced by pharmaceutical formulations during handling and device filling (Schulze, 2005). Results are presented as a flow function (derived from the inverse gradient of the graph of unconfined yield stress against consolidation stress). The higher the flow function (FF) the less cohesive the system and the more easily the powder flows.

2.4.4. Aerosolisation behaviour

Aerosolisation testing was performed on a next generation pharmaceutical impactor (NGI) with preseparator that was connected to a vacuum pump (Copley HCP5, Copley Scientific, Nottingham, UK). As NGI testing is a standard method for assessing DPI formulations, these measurements were carried out to provide information on the comparative sensitivity of the fluidised bed studies to blending-induced formulation behaviour changes. Prior to testing the preseparator was filled with 15 ml solvent, as were the NGI cups to eliminate particle bounce upon deposition. 25 ± 1 mg of each blend was accurately weighed into size 3 hydroxypropylmethyl cellulose capsules (HPMC, ShionogiQualicaps, UK). For each experiment two individual capsules of the same formulation were discharged into the NGI at 60 l min^{-1} for two bursts of 1.5 s in order to fully discharge the formulation from the device. Formulations were discharged via two separate devices; a generic sample holder made from stainless steel (Steckel and Bolzen, 2004), and a Cyclohaler® (TEVA Pharmaceuticals, The Netherlands) (Pitchayajittipong et al., 2010). Following aerosolisation, all parts of the NGI were washed with a known volume of solvent. The fine particle mass was determined by UV spectroscopy, defined as the percentage of total drug particles which deposited in stage 2 and below of the NGI (i.e. particles with aerodynamic diameters <4.64 μm).

3. Results and discussion

3.1. Effects of blending on lactose only blends

Fig. 2 shows how the particle size distribution of the lactose, as represented by two example particle size statistics, d_5 and d_{50}, changed with blending for five, typical independent blends. Table 1, which provides details of the blends produced specifically for elutriation studies (Section 3.3) gives similar information. Previously a significant increase in d_5 on blending, indicated that the fine particles in the population, in particular, are prone to blending-induced agglomeration (Bridson et al., 2007). Here, in addition

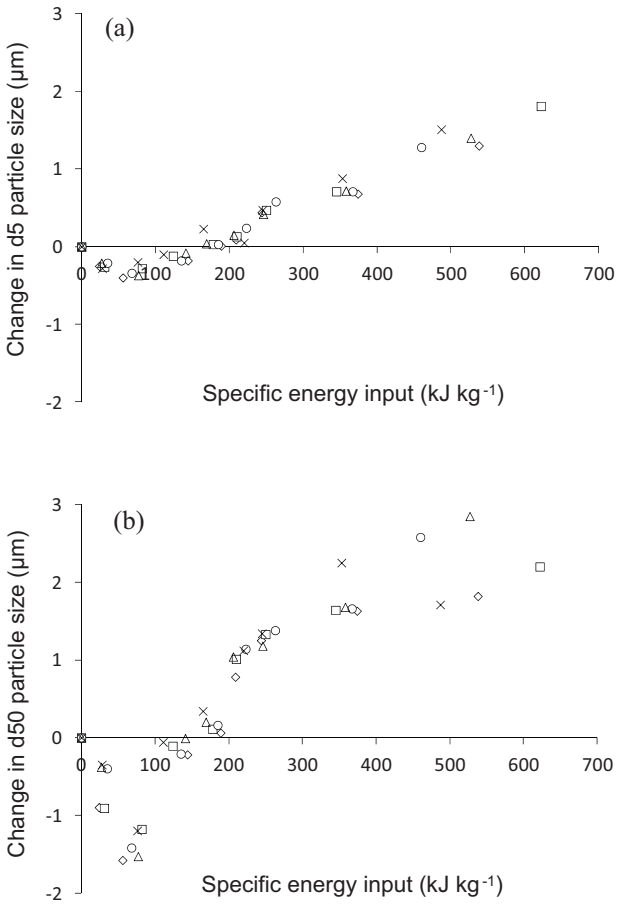

Fig. 2. Change in (a) d_5 and (b) d_{50} particle size statistics (dry laser diffraction) as a function of specific energy input. Each set of symbols corresponds to an independent blending experiment.

Table 1
Batch information for lactose used in elutriation studies. Particle size statistics were obtained from dry laser diffraction analysis and are the overall mean values from at least three samples taken from each blended batch.

Batch	Specific energy input (kJ kg^{-1})	Particle size statistics (μm)		
		d_5	d_{10}	d_{50}
Unblended				
A	0	2.97	9.72	68.7
B	0	3.03	9.59	69.5
C	0	3.06	9.93	69.0
Low energy input 1				
A	24	2.80	8.79	70.1
B	31	2.79	8.46	68.2
C	35	2.84	8.76	68.7
Low energy input 2				
A	56	2.65	8.22	67.5
B	82	2.77	8.42	67.9
C	68	2.71	8.30	67.7
Medium energy input				
A	189	3.06	9.93	69.2
B	210	3.18	10.0	70.1
C	223	3.29	10.3	70.2
High energy input				
A	538	4.35	11.5	70.9
B	622	4.86	11.8	71.3
C	460	4.33	11.6	71.7
High storage humidity				
A	N/A	5.14	13.3	75.3
B	N/A	5.20	13.5	75.4
C	N/A	5.11	13.3	75.2

to this characteristic agglomeration at high-energy inputs an earlier 'de-agglomeration' was also seen, which may be due to weak agglomerates first breaking up before continued blending causes re-agglomeration. The starting particle size distributions of the lactose batches used in the present study are different to those used by Bridson et al. (2007). In this current study, the lactose was finer particularly between the d_{10} and d_{50} region of the particle size distribution curve and this may have led to the initial de-agglomeration at lower energy inputs, which was not typically seen in the previous study.

There was no evidence to suggest that this apparent deagglomeration and subsequent re-agglomeration could be due instead to milling followed by fines 'loss' (e.g. as a result of preferential adherence of fines to the impeller or side of the bowl). In the case of material derived from the initial deagglomeration phase of three different blends, there was no statistically significant difference in specific surface area between unprocessed ($1884 \pm 124\,cm^2\,g^{-1}$) and deagglomerated material ($1954 \pm 123\,cm^2\,g^{-1}$). Similarly, wet laser diffraction analysis of lactose derived from the bulk of a blended batch, the sides of the bowl and the impeller following high energy blending ($660\,kJ\,kg^{-1}$) revealed no differences in primary particle size distribution from the original unprocessed lactose (e.g. d_{10} for unprocessed, bulk blended material and sides/impeller was $3.37 \pm 0.24\,\mu m$, $3.45 \pm 0.23\,\mu m$ and $3.40 \pm 0.14\,\mu m$, respectively; d_{50} for unprocessed, bulk blended material and sides/impeller was $56.9 \pm 1.5\,\mu m$, $57.3 \pm 2.2\,\mu m$ and $57.3 \pm 1.7\,\mu m$, respectively). Thus it appears that blending redistributes original particles, rather than resulting in the creation or loss of primary particles. In comparison to previous work (Bridson et al., 2007) it is also evident that the starting particle size distribution of the material influences whether deagglomeration or agglomeration dominates during the early stages of blending. This could have a significant impact in blend monitoring and control, particularly in the context of managing raw material variation. This in turn may impact on drug homogeneity and also drug release from the DPI as it may alter how the drug interacts with the lactose carrier particles.

3.2. Fluidisation behaviour

A classic curve is developed by measuring the pressure drop across a bed of particles as a function of increasing gas velocity. For a bed to be considered fluidised, the pressure drop across the bed should be equivalent to the bed weight per cross sectional unit area. For a readily fluidisable powder (typically low cohesivity), a linear increase in pressure drop with increasing flow rate is observed with a sharp transition from this packed bed behaviour (increasing pressure drop) to fluidised bed behaviour (static pressure drop value). A material that is difficult to fluidise (high cohesivity) will often not show the sharp transition from packed bed to fluidised bed behaviour, due to bed channelling. In extreme cases the final pressure drop value reached may not be equivalent to the weight of the bed, indicating that the powder is not fully fluidised.

Fig. 3 shows the fluidisation curves (pressure drop as a function of superficial gas velocity; ΔP vs. U_{sgv}) for a range of lactose systems, comprising three main groups: (I) inhalation grade lactose (blended and unblended; 40% RH storage); (II) sieved (coarsened) lactose, (III) lactose stored at high humidity (70% RH for 3 days). For group (I), there is no obvious difference in the fluidisation curves obtained. All showed poor initial fluidisation behaviour (i.e. bed channelling, no distinct transition from packed to fluidised bed). This is consistent with the cohesive nature of the powders, as demonstrated by their flow functions (Table 2). Interestingly, despite the obvious effects that blending has on the distribution of particles in the lactose (Fig. 2), there was no observable difference in bed behaviour or resulting fluidisation curves (Fig. 3) between unblended, low and high energy blends. It is suggested therefore

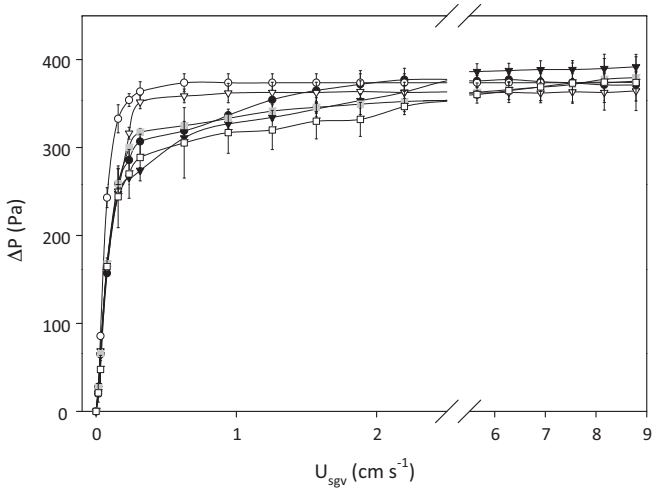

Fig. 3. Pressure drop across bed as a function of superficial gas velocity for various lactose samples. Group (I): ●, unblended lactose; ■, low energy input ($68 \pm 13\,kJ\,kg^{-1}$); ▼, high energy input ($540 \pm 81\,kJ\,kg^{-1}$); group (II): ▽, '$sieve_{71\,\mu m}$' lactose; ○, '$sieve_{25\,\mu m}$' lactose; group (III): □, high storage humidity lactose. Results shown are the overall mean from three independent blends ± standard error of the mean (s.e.m). Measurements on material from each blend were performed in triplicate.

that significant differences in fluidisation behaviour would only be observed following extreme blending regimes e.g. those that mill and generate further fines.

To further test the sensitivity of the system, samples of unblended lactose (group II) from which all particles below 25 μm ('$sieve_{25\,\mu m}$' lactose) and 71 μm ('$sieve_{71\,\mu m}$' lactose) had been removed using an Alpine Air Jet Sieve (Hosakawa Micron, Japan) were also fluidised to show how less cohesive systems (higher flow function) behaved in the fluidised bed. These curves are noticeably different to the unblended and blended lactose curves, lying above the group (I) curves, with a sharper transition from packed bed behaviour to fluidised bed behaviour. In this work, the differences in starting material, i.e. sieved vs. inhalation grade, were therefore far more significant than blending treatment in influencing fluidisation behaviour.

A further study to test if the system could distinguish between powders expected to behave differently, looked at a batch of inhalation grade lactose stored at high humidity (group III); the resulting curve was lower than for the group (I) lactose. This would be expected due to cohesivity imparted by the additional moisture content.

All systems eventually reached the same maximum value of ΔP at the flowrate of interest for the elutriation studies. This pressure drop was sufficient to support the mass of material in the bed, showing that at this point good fluidisation was achieved.

For these formulations it appears that bulk measures of fluidisation behaviour alone are unlikely to be sensitive enough to provide data of relevance to DPI blend behaviour. There is no

Table 2
Flow functions (*FF*) of powders used in this study. Results show overall average from three samples of material, three measurements on each ± s.e.m.

Material	Flow function, FF
Unprocessed lactose	3.92 ± 0.44
Mid energy blend	4.03 ± 0.53
High energy blend	4.14 ± 0.35
25 μm lactose	17.9 ± 2.0
71 μm lactose	33.2 ± 2.2
Unprocessed cholesterol	5.05 ± 0.58
Micronised cholesterol	1.94 ± 0.34

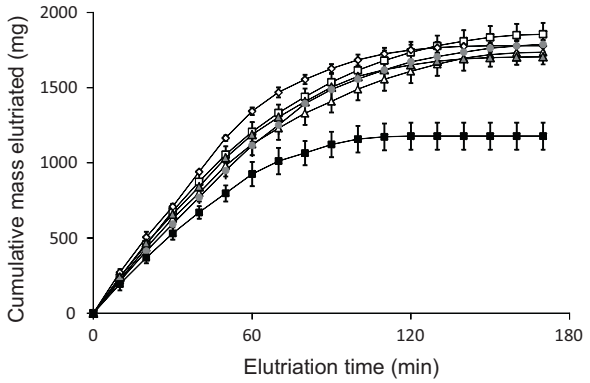

Fig. 4. Cumulative mass elutriated as a function of time for lactose subjected to various specific blend energy inputs, and deliberately agglomerated lactose. □, unprocessed lactose; ▲, low energy input 1 (30 ± 5.5 kJ kg^{-1}); ◊, low energy input 2 (68 ± 13 kJ kg^{-1}); ●, mid energy input (207 ± 17 kJ kg^{-1}); △, high energy input (540 ± 81 kJ kg^{-1}); ■, high storage humidity lactose. Results are the overall mean from three independent blends ± s.e.m. Measurements on each blend were performed in triplicate.

significant difference in fluidisation behaviour between unblended and blended material for industrially relevant energy inputs.

3.3. Elutriation behaviour

Initial tests looked at the mass of material elutriated with time (Fig. 4). From Fig. 4, it can be seen that there is minimal difference between the unblended and blended lactose. However the high humidity stored lactose showed a much lower mass of elutriated material, showing that the method can distinguish between differently processed raw materials (if the difference is large enough).

Fig. 5 shows the particle size distributions of elutriated fractions collected during fluidisation of samples from lactose-only blends subjected to varying specific energy inputs. The particle sizes corresponding to the main (largest) peak of each of the distributions are shown in Table 3. While several different sized fractions are evident for unblended lactose, blending has the effect of redistributing particles so that the fractions elutriated become more uniform. After an energy input of ~200 kJ kg^{-1}, the fractionation seen with unblended lactose is no longer apparent. Thus it appears that primary particles that contributed to the smaller fractions have agglomerated on blending and are no longer elutriated from the bed. The energy input required to create this effect corresponded well to that required to distribute a model drug homogenously within blends (Fig. 6). Energy inputs beyond this (i.e. the 'high energy' blending) had no further effect on the particle size distribution of the elutriated fractions (Table 3 and Fig. 5), the drug content of the elutriated fraction (Table 4 and Fig. 7) or the drug content uniformity of the whole blend (Fig. 6). However, the lactose was seen to continue to agglomerate with increasing energy input (Fig. 6). Whether or not such extra blending beyond that required to mix the powders is beneficial, detrimental or simply 'over-processing' and a waste of energy, depends on the effect it has on the formulation performance e.g. drug release properties. Given the known effects that lactose fines can have on the functionality of DPI formulations (e.g. Hersey, 1975; Staniforth, 1996; Lucas et al., 1998; Zeng et al., 1998; Zhou et al., 2010) the importance of applying further energy to the formulation was investigated. In this example of cholesterol plus lactose however, the extra blending had no obvious effect on the amount of drug emitted during elutriation from the fluidised bed (Fig. 7). The same conclusion could also be

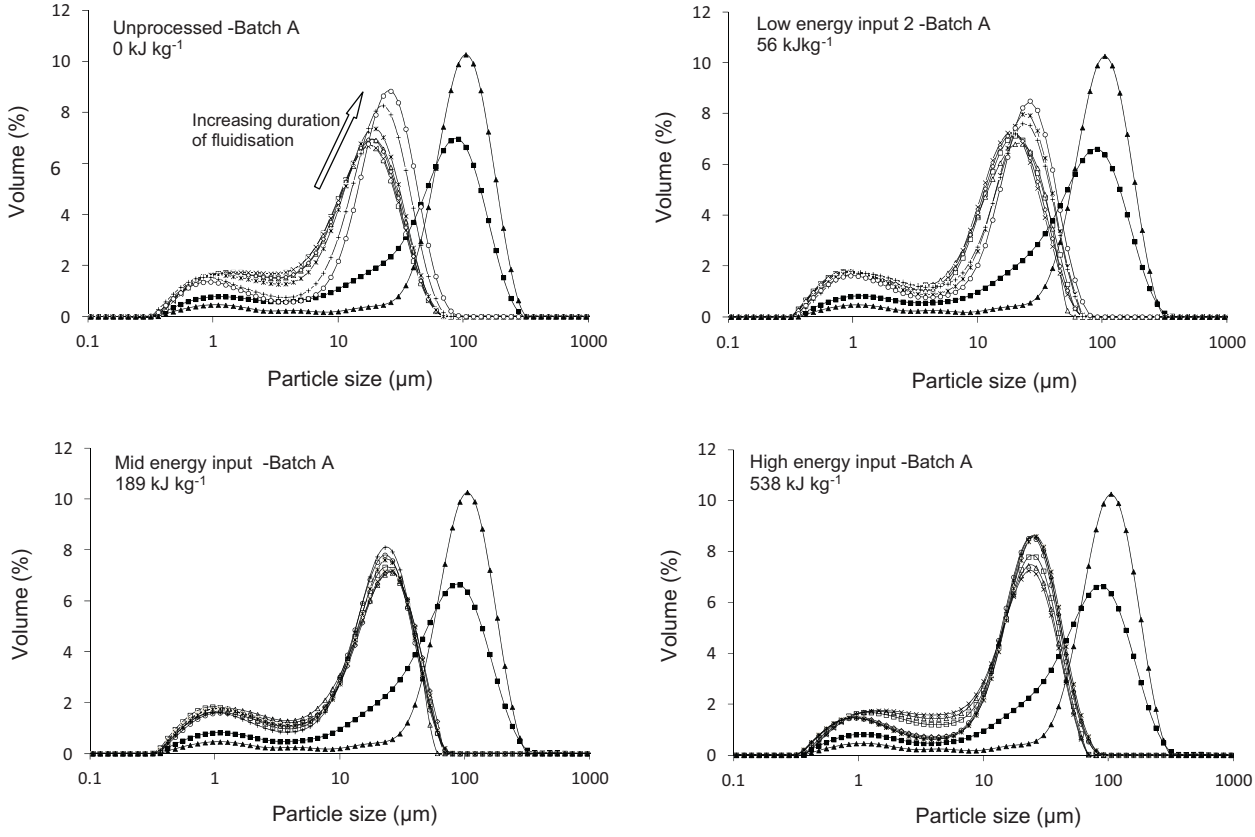

Fig. 5. Typical particle size distributions of elutriated material for a range of energy inputs. ■, bed at start; □, 10 min elutriation; △, 20 min elutriation; ×, 30 min elutriation; ◊, 50 min elutriation; ✳, 110 min elutriation; +, 120 min elutriation; ○, 130 min elutriation; ▲, bed at end.

Table 3
'Main peak' particle size values for material elutriated at different time intervals from samples subjected to varying energy inputs. Values represent the overall mean value ± s.e.m. from three independent blends at each energy input with three samples elutriated from each batch. A MATLAB code was written to find the particle size corresponding to the peak height of the particle size distribution curve. Six points around the peak of the curve were fitted to a 5th order polynomial, the peak of which was determined by integration. Trends from this data can also be seen in Fig. 5.

	"Main peak" particle size values (μm)				
	Unblended (0 kJ kg^{-1})	Low energy input 1 (30 ± 5.5 kJ kg^{-1})	Low energy input 2 (68 ± 13 kJ kg^{-1})	Mid energy input (207 ± 17 kJ kg^{-1})	High energy input (540 ± 81 kJ kg^{-1})
Non-fluidised	87.2 ± 0.60	85.7 ± 1.3	88.8 ± 0.89	86.7 ± 0.35	86.2 ± 1.8
10 min elutriation	17.8 ± 0.27	20.9 ± 0.83	18.6 ± 0.83	23.7 ± 1.2	24.6 ± 0.73
20 min elutriation	18.9 ± 1.0	19.1 ± 1.5	20.0 ± 0.59	25.3 ± 1.7	24.0 ± 1.6
30 min elutriation	18.1 ± 0.78	20.3 ± 0.71	19.3 ± 2.6	24.9 ± 1.3	23.7 ± 0.73
50 min elutriation	18.4 ± 1.4	20.8 ± 0.66	21.5 ± 1.0	25.0 ± 0.62	25.2 ± 0.69
110 min elutriation	19.2 ± 1.0	24.9 ± 1.4	24.2 ± 0.60	24.0 ± 1.9	25.8 ± 0.79
120 min elutriation	22.6 ± 0.66	24.7 ± 0.60	24.1 ± 0.93	23.6 ± 0.38	24.9 ± 0.97
130 min elutriation	25.6 ± 0.82	24.8 ± 0.84	24.1 ± 0.91	23.1 ± 1.0	24.4 ± 0.70
Average elutriation	20.1 ± 2.9	22.2 ± 2.5	21.7 ± 2.5	24.2 ± 0.84	24.6 ± 0.70
Non-elutriated	105 ± 0.83	103 ± 0.71	105 ± 1.1	106 ± 0.53	106 ± 0.88

Table 4
Particle size data, content uniformity (CV%) and fine particle mass from blended samples containing cholesterol.

SEI (kJ kg^{-1})	d_5 (μm)	d_{10} (μm)	d_{50} (μm)	CV (%)	Average drug content of sample (%)	% of drug elutriated[a]	Drug composition of elutriated fraction (%)[a]	NGI fine particle mass (%)	
								Generic	Cyclohaler
188	3.29	9.57	68.5	5.70	1.43	45.5	7.60	16.5	26.3
193	3.25	9.60	68.1	5.11	1.40	48.2	9.32	–	–
197	3.21	9.62	68.8	5.33	1.44	44.8	9.78	15.6	24.2
200	3.27	9.56	69.7	5.33	1.23	52.9	8.61	–	–
203	3.23	9.49	69.0	5.48	1.45	42.8	7.12	16.0	27.4
206	3.27	9.54	68.7	5.03	1.19	62.6	10.3	–	–
268	3.31	9.61	69.2	5.51	1.52	43.4	7.42	–	–
271	3.35	9.43	69.4	5.49	1.32	50.4	8.27	–	–
284	3.36	9.54	69.0	5.29	1.20	60.8	10.6	–	–
349	3.58	9.76	69.9	6.07	1.33	45.5	7.89	–	–
365	3.60	9.83	68.4	5.44	1.24	48.0	7.59	–	–
371	3.64	9.90	69.6	5.95	1.42	41.2	6.65	–	–
387	3.71	9.99	69.4	4.51	1.42	46.1	7.79	15.0	26.0
392	3.77	10.1	69.7	4.71	1.48	43.2	8.15	16.9	24.5
408	3.78	10.0	68.9	4.80	1.40	42.9	8.87	15.4	23.7
434	3.86	10.2	69.4	5.10	1.39	60.8	10.5	–	–
457	3.99	10.5	69.6	6.10	1.27	59.8	9.98	–	–
487	4.23	10.5	68.4	4.85	1.34	47.0	8.05	–	–
574	4.32	10.8	68.7	5.93	1.24	56.1	9.02	–	–
587	4.35	11.0	69.8	5.92	1.43	43.4	8.91	16.2	27.1
598	4.41	11.3	68.4	5.70	1.36	40.8	8.29	–	–
602	4.47	11.5	70.0	5.00	1.42	45.4	9.62	16.7	25.4
605	4.42	11.3	69.1	6.03	1.24	56.1	8.45	–	–
611	4.53	11.4	69.9	5.75	1.42	44.7	7.09	15.9	26.3

[a] Data from columns 7 and 8 are shown in Fig. 7.

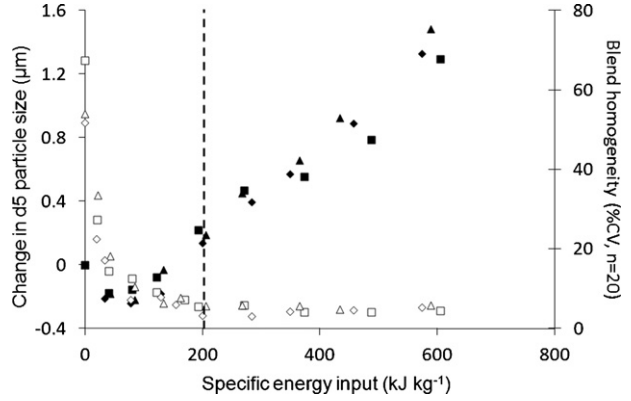

Fig. 6. Change in d_5 particle size statistic (■, ▲ and ♦) and blend homogeneity (□, △ and ◊) as a function of specific energy input for three independent 1:67.5 (w/w) cholesterol:lactose blends. The region to the right of the broken line indicates where the drug and lactose were mixed homogeneously.

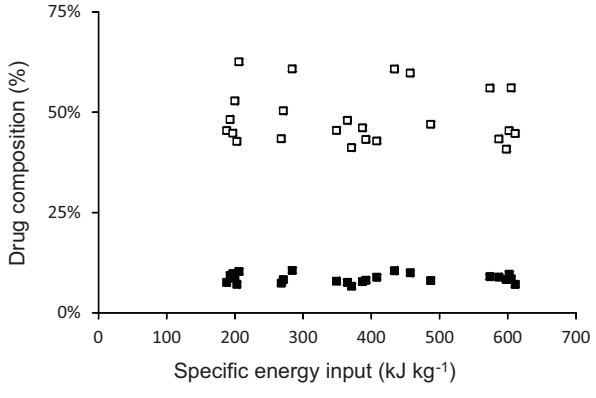

Fig. 7. Absolute drug content (%) in elutriated material (■) and emitted drug* (%) (□) as a function of specific energy input for 24 independent 1:67.5 (w/w) cholesterol:lactose blends. *NB the total emitted drug would be 100% if all drug material in the bed is elutriated. The data here show that around 50% of the drug is elutriated i.e. ~50% of the drug is still in the bed and so is not released.

drawn from the NGI data (Table 4). Thus it appears that the adhesive interactions between the cholesterol particles and the lactose carrier were developed fully during the phase of blending necessary to distribute them.

4. Conclusion

High shear blending affects the particle size distribution of lactose blends in an energy-dependent manner. These changes however do not result in differences in the bulk fluidisation behaviour of blended vs. unblended powders; only powders differing considerably in their cohesivity (i.e. 'sieved' vs. inhaled-grade in this study) can be distinguished in this way. However, characteristics of the elutriated material are a more sensitive indicator of blending-induced changes in the formulations explored and elutriation can act as a tool for identifying the extent of particle redistribution in a blend. As no further changes in the particle size distribution of the elutriated fractions are seen once the lactose and drug are well mixed, it appears that elutriation behaviour could be used as a measure of blend end-point. For this drug-lactose combination, blend energy does not affect the extent to which drug can be released from the blend as measured by both the elutriation and NGI methods employed. Initial indications are therefore that the fluidised bed method could complement existing techniques for evaluating blend behaviour and performance.

Acknowledgements

The Engineering and Physical Sciences Research Council (EPSRC) and GSK are gratefully acknowledged for providing the PhD studentship for John Willetts. The DVS Advantage II and Sympatec HELOS laser diffraction system and RODOS dispersion unit used in this research was obtained through Birmingham Science City: Innovative Uses for Advanced Materials in the Modern World (Advanced Materials 2), with support from Advantage West Midlands (AWM) and part funded by the European Regional Development Fund (ERDF).

References

Adi, H., Larson, I., Stewart, P., 2007. Laser diffraction particle sizing of cohesive lactose powders. Powder Technol. 179, 90–94.
Bridson, R.H., Robbins, P.T., Chen, Y., Westerman, W., Gillham, C.R., Roche, T.C., Seville, J.P.K., 2007. The effects of high shear blending on α-lactose monohydrate. Int. J. Pharm. 339, 84–90.
Czekai, D.A., Seaman, L.P., 1999. Method of grinding pharmaceutical substances. US Patent Number 5,862,999.
Davidson, J., Clift, R., Harrison, D., 1985. Fluidisation, 2nd ed. Academic Press, London, ISBN 0122055527.
Deng, T., Paul, K.A., Bradley, M.S.A., Immins, L., Preston, C., Scott, J.F., Welfare, E.H., 2010. Investigations on air induced segregation of pharmaceutical powders and effect of material flow functions. Powder Technol. 203, 354–358.
Flament, M.P., Leterme, P., Gayot, A., 2004. The influence of carrier roughness on adhesion, content uniformity and the in vitro deposition of terbutaline sulphate from dry powder inhalers. Int. J. Pharm. 275, 201–209.
Fournol, A.B., Bergougnou, M.A., Baker, C.G.J., 1973. Solids entrainment in a large gas fluidised bed. Can. J. Chem. Eng. 51, 401–404.
Geldart, D., 1973. Types of gas fluidisztion. Powder Technol. 7, 285–292.
Heath, T.D., Aconsky, L., 1963. Fluidised Bed Classifier. U.S. Patent Number 3,102,092.
Hersey, J.A., 1975. Ordered mixing: a new concept in powder mixing practice. Powder Technol. 11, 41–44.
Hickey, A.J., Mansour, H.M., Telko, M.J., Xu, Z., Smyth, H.D., Mulder, T., McLean, R., Langridge, J., Papadopoulos, D., 2007. Physical characterization of component particles included in dry powder inhalers. II. Dynamic characteristics. J. Pharm. Sci. 96, 1302–1319.
Jaraiz, E., Kimura, S., Levenspiel, O., 1992. Vibrating beds of fine particles: estimation of interparticle forces from expansion and pressure drop experiments. Powder Technol. 72, 22–30.
Knight, P.C., Seville, J.P.K., Wellm, A.B., Instone, T., 2001. Prediction of impeller torque in high shear powder mixers. Chem. Eng. Sci. 56, 4457–4471.
Kunii, D., Levenspiel, O., 1991. Fluidisation Engineering, 2nd ed. Butterworths, ISBN 0409902330.
Levy, E.K., Celeste, B., 2006. Combined effects of mechanical and acoustic vibrations on fluidisation of cohesive powders. Powder Technol. 163, 41–50.
Lucas, P., Anderson, K., Staniforth, J.N., 1998. Protein deposition from dry powder inhalers: fine particle multiplets as performance modifiers. Pharm. Res. 15, 562–569.
Mahmoud, E.H., Nakazato, T., Nakajima, S., Nakagawa, N., Kato, K., 2004. Separation rate of fine powders from a circulating powder-particle fluidised bed (CPPFB). Powder Technol. 146, 46–55.
Mawatari, Y., Tatemoto, Y., Noda, K., 2003. Prediction of minimum fluidisation velocity for vibrated fluidised bed. Powder Technol. 131, 66–70.
Park, A.-H., Bi, H., Grace, J.R., 2002. Reduction of electrostatic charges in gas–solid fluidised beds. Chem. Eng. Sci. 57, 153–162.
Pitchayajittipong, C., Price, R., Shur, J., Kaerger, J.S., Edge, S., 2010. Characterisation and functionality of inhalation anhydrous lactose. Int. J. Pharm. 390, 134–141.
Saint-Lorant, G., Leterme, P., Gayot, A., Flament, M.P., 2006. The influence of carrier on the performance of dry powder inhalers. Int. J. Pharm. 334, 85–91.
Santana, D., Rodrıguez, J.M., Macıas-Machın, A., 1999. Modelling fluidised bed elutriation of fine particles. Powder Technol. 106, 110–118.
Schulze, D., 2005. Flow Properties Testing with Ring Shear Testers RST-01.01, RST-01.pc and RST-XS. Schwedes + Schulze Schüttguttechnik GmbH, Braunschweig.
Shur, J., Harris, H., Jones, M.D., Kaerger, J.S., Price, R., 2008. The role of fines in the modification of the fluidisation and dispersion mechanism within dry powder inhaler formulations. Pharm. Res. 25, 1931–1940.
Smolders, K., Baeyens, J., 1997. Elutriation of fines from gas fluidised beds: mechanisms of elutriation and effect of freeboard geometry. Powder Technol. 92, 35–46.
Staniforth, J.N., 1996. Preformulation aspects of dry powder aerosols. In: Byron, P.R., Dalby, R.N., Farr, S.J. (Eds.), Respiratory Drug Delivery V. Interpharm Press, Buffalo Grove, IL, pp. 65–73.
Steckel, H., Bolzen, N., 2004. Alternative sugars as potential carriers for dry powder inhalations. Int. J. Pharm. 270, 297–306.
Thi, T.H.H., Dane, F., Descamps, M., Flament, M.-P., 2008. Comparison of physical and inhalation properties of spray-dried and micronized terbutaline sulphate. Eur. J. Pharm. Biopharm. 70, 380–388.
Tuley, R., Shrimpton, J., Jones, M.D., Price, R., Palmer, M., Prime, D., 2008. Experimental observations of dry powder inhaler dose fluidisation. Int. J. Pharm. 358, 238–247.
Zeng, X.M., Martin, G.P., Tee, S.K., Marriott, C., 1998. The role of fine particle lactose on the dispersion and de-agglomeration of salbutamol sulphate in an air stream in vitro. Int. J. Pharm. 176, 99–110.
Zenz, F.A., Weil, N.A., 1958. A theoretical-empirical approach to the mechanism of particle entrainment from fluidized beds. Am. Inst. Chem. Eng. 4, 472–479.
Zhou, Q.T., Qu, L., Larson, I., Stewart, P.J., Morton, D.A.V., 2010. Improving aerosolization of drug powders by reducing powder intrinsic cohesion via a mechanical dry coating approach. Int. J. Pharm. 394, 50–59.